Journal of Bacteriology

Expanding the Cyanuric Acid Hydrolase Protein Family to the Fungal Kingdom

Anthony G. Dodge, Chelsea S. Preiner and Lawrence P. Wackett

J. Bacteriol. **2013, 195(23):5233. DOI: 10.1128/JB.00965-13.**
Published Ahead of Print 13 September 2013.

JB
Journals.ASM.org

Expanding the Cyanuric Acid Hydrolase Protein Family to the Fungal Kingdom

Anthony G. Dodge,[a] Chelsea S. Preiner,[a] Lawrence P. Wackett[a,b]

BioTechnology Institute,[a] and Department of Biochemistry, Molecular Biology, and Biophysics,[b] University of Minnesota, St. Paul, Minnesota, USA

The known enzymes that open the *s*-triazine ring, the cyanuric acid hydrolases, have been confined almost exclusively to the kingdom *Bacteria* and are all homologous members of the rare cyanuric acid hydrolase/barbiturase protein family. In the present study, a filamentous fungus, *Sarocladium* sp. strain CA, was isolated from soil by enrichment culturing using cyanuric acid as the sole source of nitrogen. A reverse-genetic approach identified a fungal cyanuric acid hydrolase gene composed of two exons and one intron. The translated spliced sequence was 39 to 53% identical to previously characterized bacterial cyanuric acid hydrolases. The sequence was used to generate a gene optimized for expression in *Escherichia coli* and encoding an N-terminally histidine-tagged protein. The protein was purified by nickel affinity and anion-exchange chromatography. The purified protein was shown by ^{13}C nuclear magnetic resonance (^{13}C-NMR) to produce carboxybiuret as the product, which spontaneously decarboxylated to yield biuret and carbon dioxide. The protein was very narrow in substrate specificity, showing activity only with cyanuric acid and *N*-methyl cyanuric acid. Barbituric acid was an inhibitor of enzyme activity. Sequence analysis identified genes with introns in other fungi from the *Ascomycota* that, if spliced, are predicted to encode proteins with cyanuric acid hydrolase activity. The *Ascomycota* cyanuric acid hydrolase homologs are most closely related to cyanuric acid hydrolases from *Actinobacteria*.

Cyanuric acid was first synthesized in 1829 by Wöhler (1) and is currently an important commercial compound and intermediate. As examples of the latter, it is used to prepare cross-linked polymers and chlorinated cyanuric acid for disinfection. Cyanuric acid alone is only mildly toxic, but coingestion with melamine is extremely hazardous. Recently, melamine containing significant levels of cyanuric acid was used to adulterate pet food, and insoluble melamine-cyanuric acid complexes (2, 3) were identified as the etiological agents of kidney failure in animals that ingested food made with the tainted ingredients (4).

Cyanuric acid is also formed as a metabolic intermediate during the microbial metabolism of *s*-triazine compounds such as melamine (5) and the herbicide atrazine (6). This metabolic capability is found within only a very limited number of bacteria. These bacteria transform cyanuric acid to 3 mol each of ammonia and carbon dioxide (7) in a three-enzyme hydrolytic pathway. The pathway begins with cleavage of the *s*-triazine ring by the enzyme cyanuric acid hydrolase, which produces biuret (8–11). Subsequently, biuret undergoes enzymatic hydrolysis with the release of ammonia by biuret hydrolase (9, 12), and the other product, allophanate, is hydrolyzed by allophanate hydrolase (13) to produce 2 mol of ammonia and carbon dioxide, respectively.

Current knowledge of cyanuric acid hydrolase genes and enzymes is derived exclusively from studies with bacterial strains (8, 10, 11, 14–16). A recent study found 41 homologs of known cyanuric acid hydrolase genes in publicly available sequenced genomes (11). In that study, only one eukaryotic cyanuric acid hydrolase homolog, from the green alga *Micromonas* sp. strain RCC299, was found in the public databases, and it was not verified to be a bona fide cyanuric acid hydrolase.

Other enzymes that are known to cleave cyclic amide bonds belong to large protein superfamilies (17), but the cyanuric acid hydrolases are not evolutionarily related to any of these superfamilies and are relatively rare (11). Barbiturase catalyzes an analogous ring-opening reaction with the pyrimidine barbituric acid (18). The barbiturase reaction is part of the oxidative pyrimidine salvage pathway and has thus far been reported to occur only in the *Actinobacteria* (18, 19). The sequence divergence among characterized cyanuric acid hydrolases and barbiturases suggests an ancient origin for these enzymes, making it surprising that the range of reactions catalyzed by this protein family is relatively narrow (11, 14). Cyanuric acid degradation by several fungi has been described (20–23), but the genetic and enzymatic basis for degradation was not elucidated in those previous studies.

In the present study, we isolated a filamentous fungus by enrichment culturing that grew by using cyanuric acid as the sole nitrogen source. A cyanuric acid hydrolase gene homolog was identified in the strain by reverse genetics, and the translated sequence, minus the intron regions, was observed to be homologous to known bacterial cyanuric acid hydrolases. A bacterially expressible gene was designed, the encoded polypeptide was purified, and the protein was shown to catalyze cyanuric acid hydrolysis efficiently and to not act on many other analogous compounds. The hydrolysis reaction produced carboxybiuret that decomposed spontaneously to biuret, as shown by ^{13}C nuclear magnetic resonance (^{13}C-NMR). Sequence analysis revealed that this fungal protein was most closely related to other predicted fungal genes in recently deposited genome sequences and that the fungal cyanuric acid hydrolases are most closely related to bacterial cyanuric acid hydrolases from the phylum *Actinobacteria*.

Received 16 August 2013 **Accepted** 10 September 2013
Published ahead of print 13 September 2013
Address correspondence to Lawrence P. Wackett, wacke003@umn.edu.
Supplemental material for this article may be found at http://dx.doi.org/10.1128/JB.00965-13.

doi:10.1128/JB.00965-13

TABLE 1 Novel primers used in this study for PCR, RT-PCR, and sequencing

Primer	Sequence	Characteristics
Glarea130F	5′-TGYGTYAAYGAYTTYTCTCGC-3′	Degenerate PCR, forward
Glarea509R	5′-GCCATAGAYTCRTADGTRTC-3′	Degenerate PCR, reverse
SaroGSP1-5′	5′-TCAGGAGCGGGCATTTGATGA GAACCAT-3′	Genome walking, PCR, forward
SaroGSP1-3′	5′-TGCTGTAACAATATTCTCCGG CGGCACT-3′	Genome walking, PCR, reverse
SaroGSP2-5′	5′-TGTTGAGCCTGTTCGTCTGT GCCAATCT-3′	Genome walking, PCR, and sequencing, forward
SaroGSP2-3′	5′-AGATTGGCACAGACGAACAG GCTCAACA-3′	Genome walking, PCR, and sequencing, reverse
Saro-1F	5′-ATGGCGCCGATTGAGATACTC-3′	RT-PCR, forward
Saro1-1026R	5′-CTATATACTGGTCTCGTACA CCAAAC-3′	RT-PCR, reverse
Saro1-1047R	5′-TCATGATTTGTCTTCGGTGGAA-3′	RT-PCR, reverse

MATERIALS AND METHODS

Chemicals, media, and growth conditions. Commercial chemicals were obtained from Sigma-Aldrich (St. Louis, MO), except for cyanuric acid (Alfa Aesar, Heysham, United Kingdom). Ammeline (2,4-diamino-6-hydroxy-1,3,5-triazine); ammelide (2-amino-4,6-dihydroxy-1,3,5-triazine); methyl-, 1,3-dimethyl-, and trimethylisocyanuric acids; 5-nitro barbituric acid; and 5-methyl barbituric acid were synthesized in our laboratory as described previously (24, 25). Enrichment cultures and isolated strains were grown at 28°C in nitrogen-free basal salts (NFB) medium composed of 50 mM potassium phosphate buffer (pH 7.0) supplemented with magnesium, calcium, trace elements, and vitamins (26). Carbon sources were added to 0.2% as noted, and nitrogen sources were added to provide 3.0 to 9.0 mM available nitrogen atoms. Liquid cultures were shaken at 225 rpm. Cyanuric acid clearing plates were prepared by adding an oversaturating amount (1.75%) of cyanuric acid into NFB medium with 1.5% Noble agar. *Escherichia coli* cultures were grown at 37°C in LB medium supplemented with 50 μg/ml kanamycin when required.

Nucleic acid isolation and manipulations. Total genomic DNA and RNA were purified from fresh biomass that was ground under liquid nitrogen with a mortar and pestle. Genomic DNA was isolated with a DNeasy plant minikit, and total RNA was isolated with an RNeasy minikit (Qiagen, Hilden, Germany). Purified nucleic acids were quantitated with a NanoDrop 2000 instrument (Thermo Scientific, Wilmington, DE). PCRs were conducted with Phusion polymerase (New England BioLabs Inc., Ipswich, MA), unless noted otherwise. A Qiagen OneStep reverse transcriptase PCR (RT-PCR) kit was used for RT-PCR. Cycling conditions used were those recommended by the manufacturers. Novel primers used for PCR, RT-PCR, and sequencing are listed in Table 1. PCR-amplified fragments were purified with a Qiagen QIAquick gel extraction kit. Gel-purified PCR products were cloned with a StrataClone PCR cloning kit (Agilent Technologies, Santa Clara, CA) and sequenced with primers M13 and M13-20 or with gene-specific primers as described below. Sanger DNA sequencing was done by ACGT Inc. (Wheeling, IL).

Enrichment culturing, strain isolation, and strain identification. Enrichment cultures were started by adding 1.0 g of soil from a campus garden into 25 ml NFB medium with 1.0 mM cyanuric acid as the sole nitrogen source and with glucose, sodium acetate, sodium succinate, glycerol, and sodium citrate as carbon sources. The culture was transferred at 48- to 72-h intervals by inoculating a new aliquot of medium with 4 to 20% of the previous culture. Serial dilutions of the fifth-transfer culture were spread onto cyanuric acid clearing plates and incubated. Colony types that showed cyanuric acid clearing were streaked onto separate plates and incubated. Colony types that showed clearing in isolation were then tested for growth alone in the enrichment medium. Cyanuric acid degradation was confirmed by monitoring the UV absorbance of culture supernatants with a Beckman-Coulter (Brea, CA) DU-640 spectrophotometer. Isolates were further characterized by rRNA gene sequencing. A 1,724-bp fragment from the nuclear small-subunit (18S) rRNA gene was amplified with primers NS1 and NS8 and sequenced with primers NS1, NS2, NS7, and NS8 (27); a 541-bp fragment spanning internal transcribed spacer 1 (ITS1), ITS2, and the 5.8S rRNA gene was amplified and sequenced with primers ITS1 and ITS4 (27).

DNA and protein sequence alignments and creation of phylogenetic trees. DNA sequences were aligned against the nucleotide collection in GenBank (Bethesda, MD) by using BLAST (28). Routine alignments of protein sequences were done with ClustalW (29). MEGA 5 (30) was used to align protein sequences with MUSCLE (31) and to generate maximum likelihood and neighbor-joining phylogenetic trees. A consensus maximum likelihood tree was generated from 500 bootstrap replicates. The GI numbers of the sequences used to create the phylogenetic trees are presented in Table S1 in the supplemental material.

Anion-exchange chromatography to fractionate cyanuric acid hydrolase activity. *Sarocladium* sp. strain CA was grown in 2,000 ml of NFB medium with 0.2% glucose and 3 mM cyanuric acid as the sole nitrogen source, harvested with a 150-ml, 0.2-μm-mesh surfactant-free cellulose acetate (SFCA) membrane bottle-top filter (Nalgene, Rochester, NY), and ground for 5 min in a chilled mortar and pestle with 2 ml cold 20 mM Bis-Tris buffer (pH 7.0) (binding buffer) 1.0 g of 3M Empore Filter Aid 400 high-density glass beads (Fisher Scientific, Pittsburgh, PA) per g wet biomass. The slurry was centrifuged in chilled microcentrifuge tubes at 14,000 rpm for 15 min at 4°C. Supernatants were passed through an Acrodisc 0.45-μm HT Tuffryn membrane syringe filter (Pall Corporation, Ann Arbor, MI), and the filtrate (5.5 ml) was mixed with 6.0 ml of a DEAE-Sephadex A50 anion-exchange resin slurry in binding buffer. The mixture was swirled periodically and kept on ice in a cold room for 1 h. Unbound proteins were collected by washing the resin four times with 1 volume of binding buffer and harvesting the supernatants by filtration as described above. Bound proteins were eluted by similarly washing the resin with binding buffer plus potassium chloride (KCl) added to 0.1, 0.2, or 0.3 M. The first wash fractions from each elution step were concentrated 10 times by using Millipore Amicon Ultra-15 centrifugal filters (10,000 nominal molecular weight limit [NMWL]) (Billerica, MA). Protein concentrations were determined by using Bio-Rad (Hercules, CA) protein assay reagent (32). Fractions were screened for cyanuric acid hydrolase activity by adding 5 to 20 μg protein from the first wash fractions to 1.0 ml of 3 mM cyanuric acid in potassium phosphate buffer (pH 7). The reaction mixtures were incubated overnight and then diluted 20× for UV spectroscopy analysis. Cyanuric acid hydrolase activity was indicated by a decrease in absorbance of the cyanuric acid peak at 214 nm.

Protein mass spectrometry. The first 0.2 M KCl elution fraction was submitted for peptide analysis to the University of Minnesota Center for Mass Spectrophotometry and Proteomics. Proteins (3.4 μg) were digested in solution with trypsin (Promega, Madison, WI), and the peptides were desalted with 3M Empore styrenedivinylbenzene (SDB) filter paper according to the stage tip procedure (33), dried, dissolved in 5.5 μl of water-acetonitrile-formic acid (98:2:0.01), loaded onto a 12-cm- by 75-μm-diameter fused silica pulled-tip capillary column packed with Magic C_{18AQ} reversed-phase resin (New Objective Inc., Woburn, MA), and eluted with a 10 to 40% gradient of acetonitrile-water-formic acid (98:2:0.01). Peptides were then analyzed by online capillary LC-nanoESI-MS/MS (liquid chromatography-nanoscale electrospray ionization-tandem mass spectrophotometry) using a Velos Orbitrap mass spectrophotometer (Thermo Fisher) with HCD (high-energy-collision-induced dissociating) activation, as previously described (34).

ProteinPilot 4.2 (AB Sciex, Framingham, MA) was used to find exact peptide matches in a database composed of 41 cyanuric acid hydrolase homologs (11); protein sequences from the order *Hypocreales* and the fungal genera *Aspergillus*, *Penicillium*, and *Sporothrix* downloaded from GenBank; plus a database of common contaminant proteins from the Global Proteome Machine (http://www.thegpm.org/crap/index.html). Additional peptides in the sample that were homologous but not identical

to peptides in the database were inferred by *de novo* sequencing with PEAKS version 5.3 software (Bioinformatics Solutions, Waterloo, Ontario, Canada).

Gene prediction and identification. Peptide sequences obtained by mass spectrometry were used to design degenerate PCR primers with GeneFisher2 (35) on the BiBiServ server (http://bibiserv.techfak.uni-bielefeld.de/genefisher2/). The primers were used in RT-PCRs with total RNA from the fungal isolate as the template. The sequence of the amplified fragment was extended in both directions by DNA sequence walking with a GenomeWalker Universal kit (Clontech, Mountain View, CA) and primers SaroGSP1-5′, SaroGSP1-3′, SaroGSP2-5′, and SaroGSP2-3′ (Table 1). Potential genes were predicted in the resulting sequence on the Softberry Inc. server, using the FGENESH (HMM-based gene structure prediction) and FGENESH$^+$ (HMM plus similar protein-based gene prediction) programs with *Penicillium* as the model genus and the *Rhodococcus* sp. strain Mel cyanuric acid hydrolase (16) as the model protein sequence, respectively. A cyanuric acid hydrolase gene was similarly predicted in the *Glarea lozoyensis* ATCC 74030 genomic sequence using *Botrytis* as the model genus. RT-PCR was used with primer Saro-1F paired with primer Saro1-1026R or Saro1-1047R to verify the correct stop codon and sequence of the predicted spliced transcript in the fungal isolate.

Gene cloning, protein expression, and protein purification. The predicted cyanuric acid hydrolase gene from the isolate was codon optimized for expression in *E. coli* by DNA 2.0 (Menlo Park, CA). The synthetic gene was cloned into a pET28b+ vector as an NdeI-EcoRI fragment so that the expressed polypeptide would have an N-terminal six-His tag. Protein expression was induced with 0.1 mM isopropyl-β-D-thiogalactopyranoside (IPTG) in *E. coli* BL21(DE3) cells grown in LB plus kanamycin, as described previously (10). Cells were resuspended in 0.1 M potassium phosphate buffer (pH 7.0) containing 20 mM imidazole and 0.2 M sodium chloride (buffer A), lysed with a French press, centrifuged as described previously (10), and then filtered with Acrodisc 0.45-μm HT Tuffryn syringe filters. The filtered lysate was loaded onto a HisTrap HP 5-ml column charged with $NiSO_4$ and connected to an Äkta fast protein liquid chromatography (FPLC) system (GE Healthcare, Piscataway, NJ). The column was washed with 10% buffer B (buffer A with 0.5 M imidazole), and the remaining bound proteins were eluted with a linear gradient (20 column volumes) from 10% to 100% buffer B. Fractions containing the peak that eluted from 43% to 90% buffer B were pooled, and the buffer was exchanged to binding buffer by using Amicon Ultra-15 filters. The protein solution was then loaded onto a column packed with Bio-Rad Macro-Prep DEAE weak-anion-exchange resin, the column was washed with 0.1 M KCl, and the remaining bound proteins were eluted with a linear gradient (20 column volumes) from 0.1 to 0.3 M KCl in the binding buffer. Fractions containing the peak that eluted from 0.11 to 0.16 M KCl were pooled and concentrated as described above. Purity was checked by SDS-PAGE, and the identity of protein bands was confirmed by mass spectrometry.

Enzyme assays, determination of kinetic constants, and identification of reaction products. Assays to determine kinetic constants were conducted at pH 8.0 with 10 to 2,000 μM cyanuric acid and 1 to 5 μg enzyme. A real-time spectrophotometric assay in 25 mM Tris-HCl (10) was used at substrate concentrations of ≤100 μM ($\varepsilon = 9{,}200\ cm^{-1}\ M^{-1}$). A fixed-time-point ammonia detection assay was used to determine reaction rates at higher substrate concentrations in 25 mM potassium phosphate. Catalysis was stopped by boiling reaction tubes for 10 min, tubes were cooled to room temperature, and 3 μg of purified biuret hydrolase (12) was added. After 1 h, ammonia concentrations were determined by using the Berthelot reaction (36). Products produced by enzymatic reactions were monitored by nuclear magnetic resonance (NMR) spectroscopy using universally labeled [^{13}C]cyanuric acid, as described previously (11). Activity on 100 μM *N*-methylisocyanuric acid was determined by a spectrophotometric assay as described above ($\varepsilon = 9{,}500\ cm^{-1}\ M^{-1}$). Activity on other potential substrates (cytosine, 5-azacytosine, thymine, uracil, 5,6-dihydroxyuracil, 2,4,5-trihydroxy-pyrimidine, 6-azauracil, ammeline, ammelide, 2-isopropylamino-4,6-dihydroxy-*s*-triazine, 2,4-dioxohexahydro-*s*-triazine, 2,4,6-trimethoxy-1,3,5-triazine, methylisocyanuric acid, 2,3-dimethylisocyanuric acid, trimethylisocyanuric acid, trithiocyanuric acid, barbituric acid, 5-nitrobarbituric acid, 5-methylbarbituric acid, hydantoin, succinamide, and maleimide) was screened by checking for UV spectrum changes after incubation of 100 μM substrate with 25 μg of enzyme overnight. Competitive inhibition assays were conducted via the spectrophotometric assay with 100 μM cyanuric acid plus 0.125, 0.25, or 0.5 μM barbituric acid and 5 μg of enzyme.

Nucleotide sequence accession numbers. The 18S rRNA and ITS/5S rRNA sequences were submitted to GenBank under accession numbers KF537244 and KF537245, respectively. The sequence of the contig containing the *Sarocladium* sp. CA cyanuric acid hydrolase gene was submitted to GenBank under accession number KF537246.

RESULTS AND DISCUSSION

Isolation and identification of a cyanuric acid-degrading fungus. An enrichment culture on cyanuric acid was plated onto opaque agar plates oversaturated with cyanuric acid to give a single colony type that cleared insoluble cyanuric acid on the plates. The peach-colored colonies consisted of a filamentous organism that showed septate hyphae, cylindrical/ellipsoid conidia, and chlamydospores, indicating that it was a fungus. The ITS and 5.8S subunit sequence (541 nucleotides [nt]) were 100% identical to several sequences from fungal genera that included *Sarocladium*, *Acremonium*, *Nectria*, and *Sigmoidea*. The small-subunit rRNA gene sequence was 100% identical (1,724/1,724 nt) to the *Sarocladium kiliense* strain CBS 122.29 sequence and was highly similar (1,723/1,724 nt) to the *Sarocladium kiliense* strain CBS 146.62 and *Sarocladium bactrocephalum* strain CBS 749.69 sequences. Because these strains were members of a recently defined *Sarocladium* species clade (37), the isolate was assigned to this genus and denoted *Sarocladium* sp. CA.

Identification of the cyanuric acid hydrolase homolog of *Sarocladium* sp. CA. A reverse-genetics approach was used to identify the cyanuric acid hydrolase activity as a prelude to identifying the gene (Fig. 1). First, a cell-free protein extract was prepared and subjected to anion-exchange chromatography, and cyanuric acid hydrolase activity was detected in the 0.2 M KCl eluate, which contained a significant number of protein bands (Fig. 2A). The protein fraction obtained was treated with trypsin protease, and the peptides were analyzed by MS/MS. The peptide sequences were then compared to those of proteins found in fungal genome projects, bacterial cyanuric acid hydrolases, and common contaminant proteins. Surprisingly, a 12-residue peptide (TEGNGC VNDFSR) (Fig. 2B) that exactly matched a peptide sequence contained within a cyanuric acid hydrolase from the bacterium *Azorhizobium caulinodans* ORS571 (locus AZC_3892) was found. Attempts to amplify the cyanuric acid hydrolase gene sequence from *Sarocladium* sp. CA using degenerate PCR primers designed from this peptide and other regions conserved among cyanuric acid hydrolase homologs were not successful. To identify additional peptides that were similar, but not identical, to the tryptic peptides in the database, peptide sequences were generated from the MS/MS data by *de novo* sequencing independent of the database. This method inferred seven peptides ranging in length from 5 to 18 residues, a representative member of which is shown in Fig. 2C.

PCR amplification of cyanuric acid hydrolase gene regions from *Sarocladium* sp. CA genomic DNA was attempted with degenerate primers designed from the peptide sequences identified

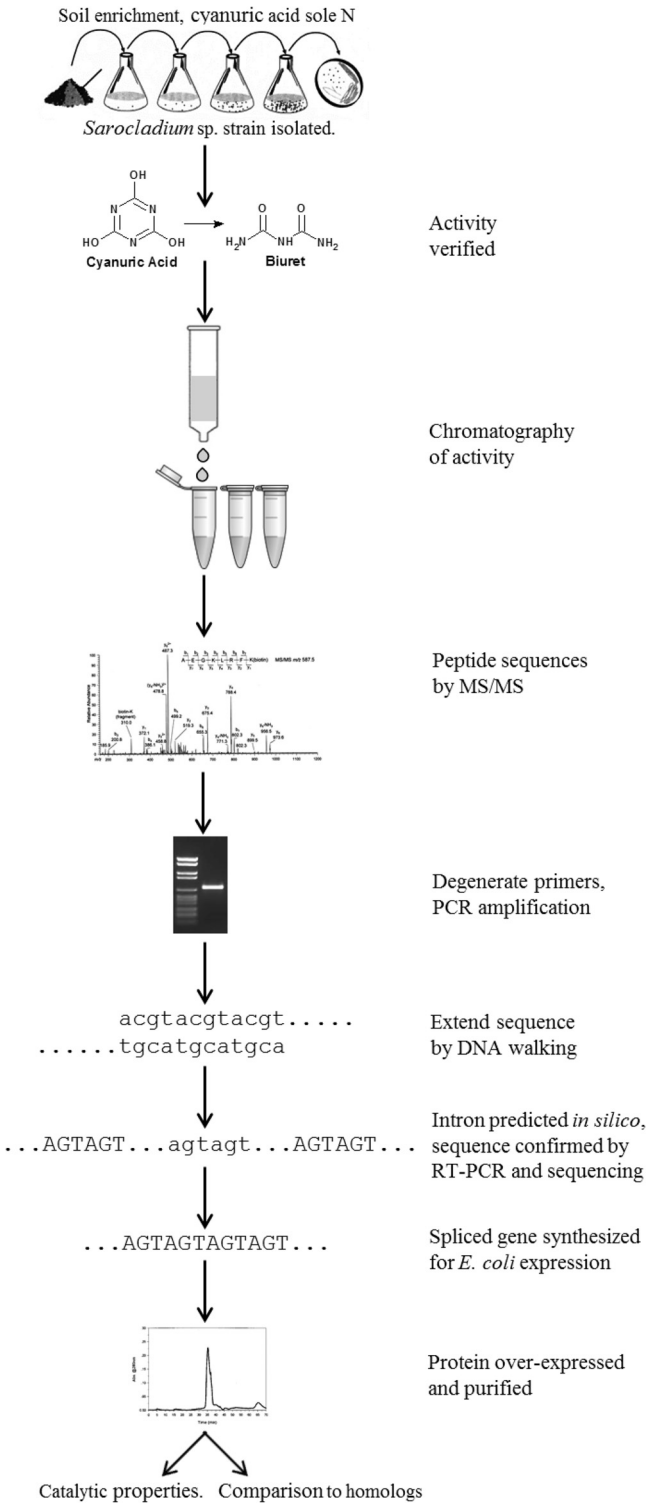

FIG 1 Schematic showing the experimental steps from enrichment culturing to gene discovery, protein purification, and protein characterization.

by MS/MS. Primers 130F and 590R, designed from the 12-residue peptide (Fig. 2B) and a 13-residue peptide inferred by *de novo* sequencing (VPVTTDTYESMAR) (Fig. 2C), amplified a 345-bp fragment (386 bp including the primer annealing regions) that could be translated into a 115-amino-acid (aa) polypeptide. When the sequence was aligned against nonredundant protein sequences in GenBank, the top matches were all proteins within the cyanuric acid hydrolase/barbiturase family. Sequence walking extended the nucleotide sequence in both directions, ultimately yielding a 1,666-nt contig. BLAST alignment of the translated sequence revealed two open reading frames (ORFs) that were homologous to cyanuric acid hydrolase sequences but that were not contiguous and were in different reading frames.

Confirmation of exons and introns in the *Sarocladium* gene and identification of other eukaryotic cyanuric acid hydrolase gene homologs. To identify potential introns within the contig, the sequence was analyzed with gene prediction programs using other fungal sequences as models. Three versions of a single gene were predicted within the contig, consisting of two or three exons and one or two introns, respectively. To determine the authentic spliced sequence of the gene transcript, RT-PCR was conducted with reverse primers specific to the predicted 3′ termini and total RNA from *Sarocladium* sp. CA as the template. Amplification was observed only with the primer set designed to amplify the two-exon genes. The sequence of the amplified product was 100% identical to that of the predicted spliced transcript of the two-exon gene shown in Fig. 3A. In pairwise alignments, identities between the putative *Sarocladium* sp. CA sequence and known functional cyanuric acid hydrolases ranged from 39 to 53%, whereas the pairwise identities among bacterial cyanuric acid hydrolase sequences ranged from 40 to 60% (Table 2). Similar tools allowed the identification of several other likely fungal cyanuric acid hydrolase genes and their coding regions (Fig. 3B).

Two cyanuric acid hydrolase/barbiturase family homologs were also discovered in the genome of the eukaryotic photosynthetic plankton *Emiliania huxleyi* CCMP1516. The predicted *Emiliania* proteins were composed of 373 or 797 aa. The shorter polypeptide (EMIHUDRAFT_196547) was encoded by a single ORF with no introns. The 797-aa polypeptide (EMIHUDRAFT_464926) was predicted to be encoded by a 2,394-nt gene composed of 4 exons (1,118, 606, 380, and 342 nt) and 3 introns (312, 78, and 72 nt). This polypeptide appeared to be a fusion of an N-terminal cyanuric acid hydrolase family domain with an aspartyl/asparaginyl beta-hydroxylase superfamily domain. However, there was an in-frame stop codon that began 2 nt downstream of the first exon. The polypeptide encoded by this ORF was the same length as EMIHUDRAFT_196547, and alignment of the two sequences revealed that 371 aa of 373 aa were identical, implying that a gene duplication event had occurred.

Protein purification and identification of the protein as a functional cyanuric acid hydrolase. The spliced gene sequence was synthesized with codons optimized for expression in *E. coli*. The encoded polypeptide was overexpressed with an N-terminal six-His tag and purified to near homogeneity. The activity of the enzyme was screened with a continuous spectrophotometric assay that showed depletion of the cyanuric acid peak at 214 nm. In a separate experiment, reacting 150 nmol of cyanuric acid with the fungal protein plus biuret hydrolase enzyme yielded 142 nmol of ammonia, indicating that the fungal enzyme ultimately produced biuret from cyanuric acid as do bacterial cyanuric acid hydrolases (8, 11, 38).

To verify that the fungal cyanuric acid hydrolase reaction followed the same reaction mechanism as the bacterial enzymes, initial reaction products released from the enzyme were monitored

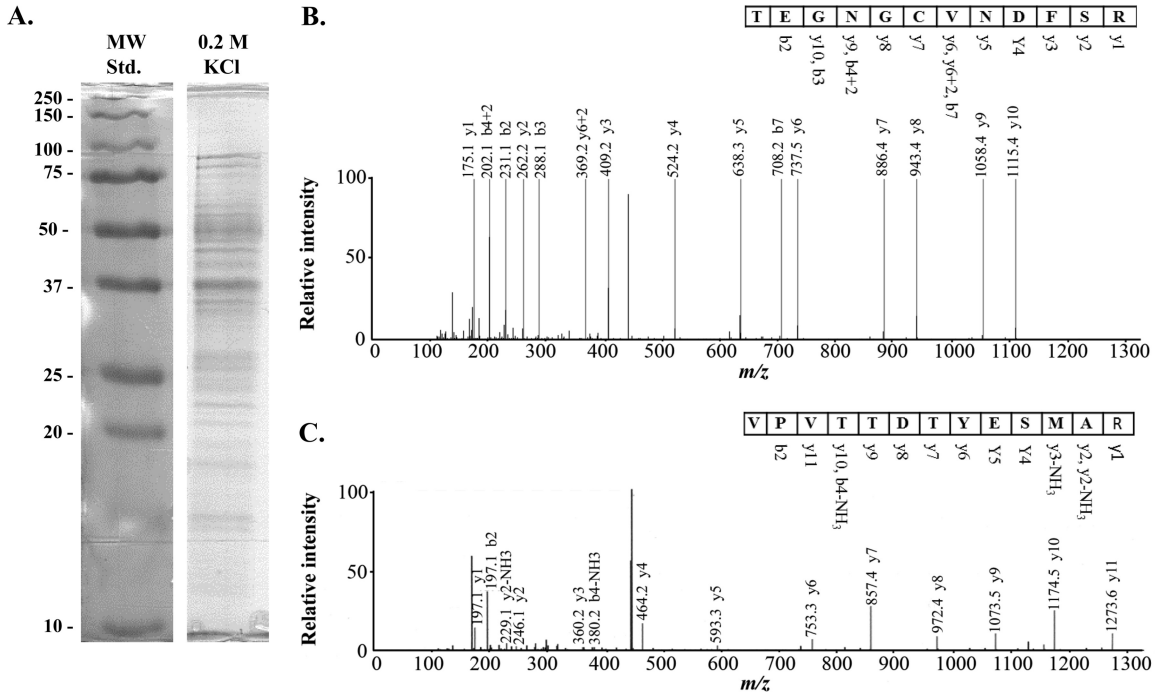

FIG 2 Fractionation of cyanuric acid hydrolase activity from a *Sarocladium* sp. crude cell extract and MS/MS identification of cyanuric acid hydrolase peptide homologs. (A) SDS-PAGE analysis of the fraction with cyanuric acid hydrolase activity that was eluted from DEAE resin with 0.2 M KCl. MW, molecular weight (in thousands). (B and C) Mass spectra of two cyanuric acid hydrolase peptide homologs identified in the active fraction by database matching (B) or *de novo* sequencing (C). The y and/or b ions that identified each residue are indicated.

in real time by starting with ^{13}C-labeled cyanuric acid and monitoring the reaction by ^{13}C-NMR. Within minutes, the cyanuric acid resonance at 157.3 ppm largely disappeared, with the subsequent appearance of three resonances with chemical shifts of 157.1, 156.8, and 155.0 ppm (Fig. 4A), which were previously shown to be characteristic of carboxybiuret (11, 12). The three resonances were transient, consistent with a rapid decarboxylation of carboxybiuret to form biuret and bicarbonate, showing chemical shifts of 157.5 and 160.3 ppm, respectively (Fig. 4B). The formation of carboxybiuret as the direct enzyme product, followed by spontaneous decarboxylation to biuret, has also been observed in reaction mixtures of the bacterial cyanuric acid hydrolases (11, 12).

While the above-described studies clearly showed that the fungal enzyme had cyanuric acid hydrolase activity, it was possible that it was active with other substrates and that those

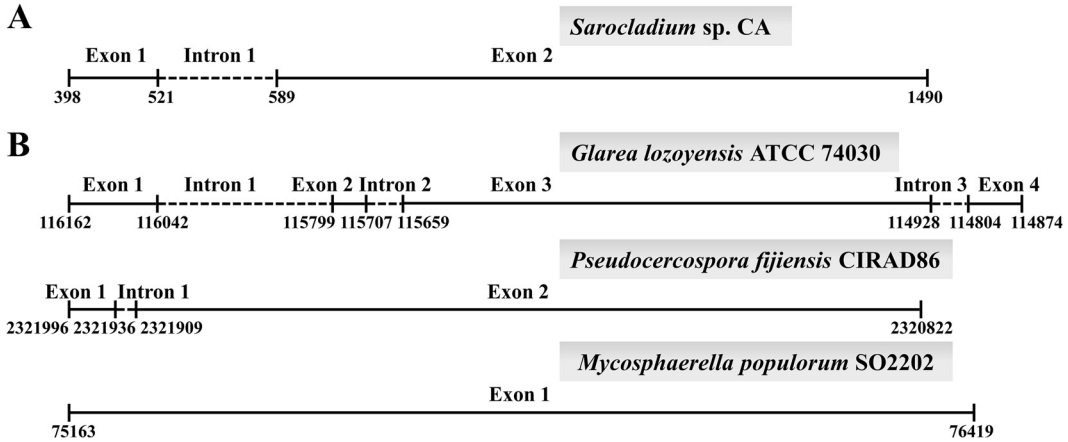

FIG 3 Exon (solid lines) and intron (dashed lines) structures of confirmed and predicted fungal cyanuric acid hydrolase family genes (lengths are proportional). Nucleotide positions of exon boundaries are indicated. (A) The *Sarocladium* sp. CA authentic splicing pattern, as confirmed by RT-PCR. (B) The *G. lozoyensis* ATCC 74030 gene was predicted in the unannotated genomic sequence in GenBank (GI:361128271). The *Pseudocercospora fijiensis* CIRAD86 gene was annotated in GenBank (GI:452984457) as encoding a hypothetical protein in the cyanuric acid hydrolase family. The *Mycosphaerella populorum* SO2202 gene was predicted from a two-exon gene annotated in GenBank as encoding a hypothetical fusion protein with an N-terminal cyanuric acid hydrolase family domain (GI: 453082292). The single exon version shown above uses an in-frame stop codon that was identified with the FGENESH algorithm on the Softberry server.

TABLE 2 Pairwise comparison by BLAST analysis of functional cyanuric acid hydrolases and barbiturase

Protein or source strain genus	% aa sequence identity to other functional cyanuric acid hydrolases								
	AtzD	TrzD	*Moorella*	*Bradyrhizobium*	*Rhizobium*	*Methylobacterium*	*Azorhizobium*	Barbiturase	*Rhodococcus*
Sarocladium	43	40	42	42	44	39	41	35	53
Rhodococcus[a]	43	40	43	45	45	42	44	38	100
Barbiturase[b]	44	48	49	44	44	38	41	100	
Azorhizobium[c]	51	52	55	54	57	58	100		
Methylobacterium[d]	47	47	48	47	44	100			
Rhizobium[e]	49	51	53	52	100				
Bradyrhizobium[f]	61	57	59	100					
Moorella[g]	58	64	100						
TrzD[h]	58	100							
AtzD[i]	100								

[a] *Rhodococcus* sp. Mel (16).
[b] *Rhodococcus erythropolis* JCM 3132 (18).
[c] *Azorhizobium caulinodans* ORS571 (11).
[d] *Methylobacterium* sp. strain 4-46 (11).
[e] *Rhizobium leguminosarum* bv. viciae 3841 (11).
[f] *Bradyrhizobium japonicum* USDA 110 (11).
[g] *Moorella thermoacetica* ATCC 39073 (10).
[h] *Acidovorax citrulli* strain 12227 (8).
[i] *Pseudomonas* sp. ADP (9, 14).

substrates might be more important physiologically. In this context, the purified fungal enzyme was screened for activity on several triazine and pyrimidine analogs. No activity was detected with the following compounds: cytosine, 5-azacytosine, thymine, uracil, 5,6-dihydroxyuracil, 2,4,5-trihydroxy-pyrimidine, 6-azauracil, ammeline, ammelide, 2-isopropylamino-4,6-dihydroxy-*s*-triazine, 2,4-dioxohexahydro-*s*-triazine, 2,4,6-trimethoxy-1,3,5-triazine, *N*,*N*-dimethylisocyanuric acid, *N*,*N*,*N*-trimethylisocyanuric acid, trithiocyanuric acid, barbituric acid, 5-nitrobarbituric acid, 5-methylbarbituric acid, hydantoin, succinamide, and maleimide. Besides cyanuric acid, activity was detected only on *N*-methylisocyanuric acid. The specific activity of the fungal enzyme with 100 μM *N*-methylisocyanuric acid was 69% of the activity with 100 μM cyanuric acid. A similar relative activity with *N*-methylisocyanuric acid was reported for AtzD, the cyanuric acid hydrolase from *Pseudomonas* sp. strain ADP (14). The *Moorella thermoacetica* ATCC 39073 cyanuric acid hydrolase showed <1% of the activity on *N*-methylisocyanuric acid as it did with cyanuric acid (10).

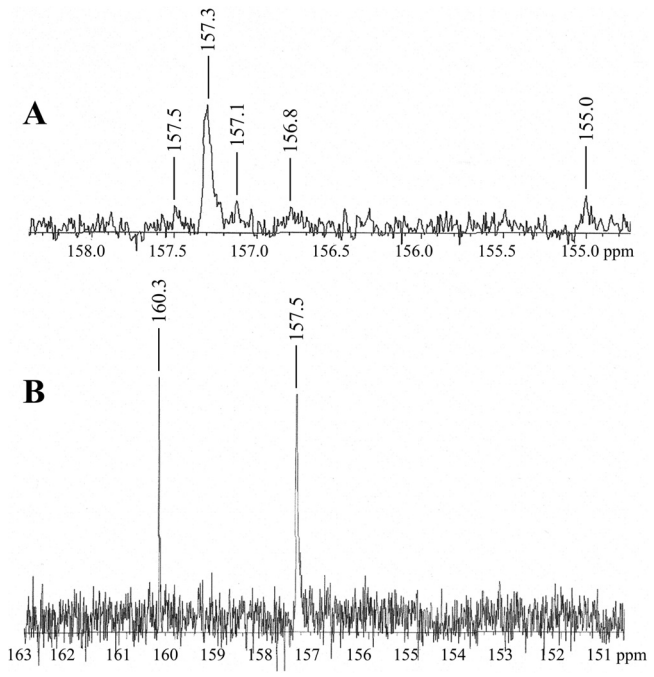

FIG 4 ^{13}C-NMR analysis of ^{13}C-labeled cyanuric acid hydrolysis by the *Sarocladium* sp. CA cyanuric acid hydrolase. Shown is the composite spectrum acquired immediately after addition of the enzyme (A) and the composite spectrum acquired the next day (B).

Steady-state kinetics and inhibition. Steady-state kinetic assays gave a k_{cat} of 3.4 ± 0.2 s^{-1} and a K_m of 400 ± 55.7 μM. The k_{cat}/K_m value was thus approximately 10^4 M^{-1} s^{-1}. The parameters measured with the fungal enzyme were lower than those reported for several characterized bacterial enzymes (4×10^4 M^{-1} s^{-1} to 10^6 M^{-1} s^{-1}), but they were not far outside the range.

Barbituric acid was tested as an inhibitor at concentrations of 0.125, 0.250, and 0.500 μM in 100 μM cyanuric acid. Specific activities in the presence of different levels of barbituric acid were 58, 30, and 17%, respectively, of the activity observed with the substrate but lacking the inhibitor. Barbituric acid was previously shown to be a strong competitive inhibitor of the cyanuric acid hydrolases AtzD (14) and TrzD (8).

Phylogeny of *Sarocladium* cyanuric acid hydrolase and other cyanuric acid hydrolases. A phylogenetic tree (maximum likelihood) was generated to infer evolutionary relationships among the cyanuric acid hydrolase/barbiturase homologs in GenBank and the newly discovered eukaryotic homologs (Fig. 5). The analysis was done with 79 sequences (the 7 eukaryotic sequences plus 72 complete sequence homologs from GenBank), and the tree was rooted with the *Frankia* sp. strain EuI1c sequence (GI:280963003) (Fig. 5), as was done previously (11).

The four fungal sequences clustered together (Fig. 5). The *Sarocladium* sp. CA sequence was most closely related to the predicted *Glarea lozoyensis* ATCC 74030 sequence (Fig. 3B). The four fungal sequences shared a node with three actinobacterial sequences, including the functional cyanuric acid hydrolase from

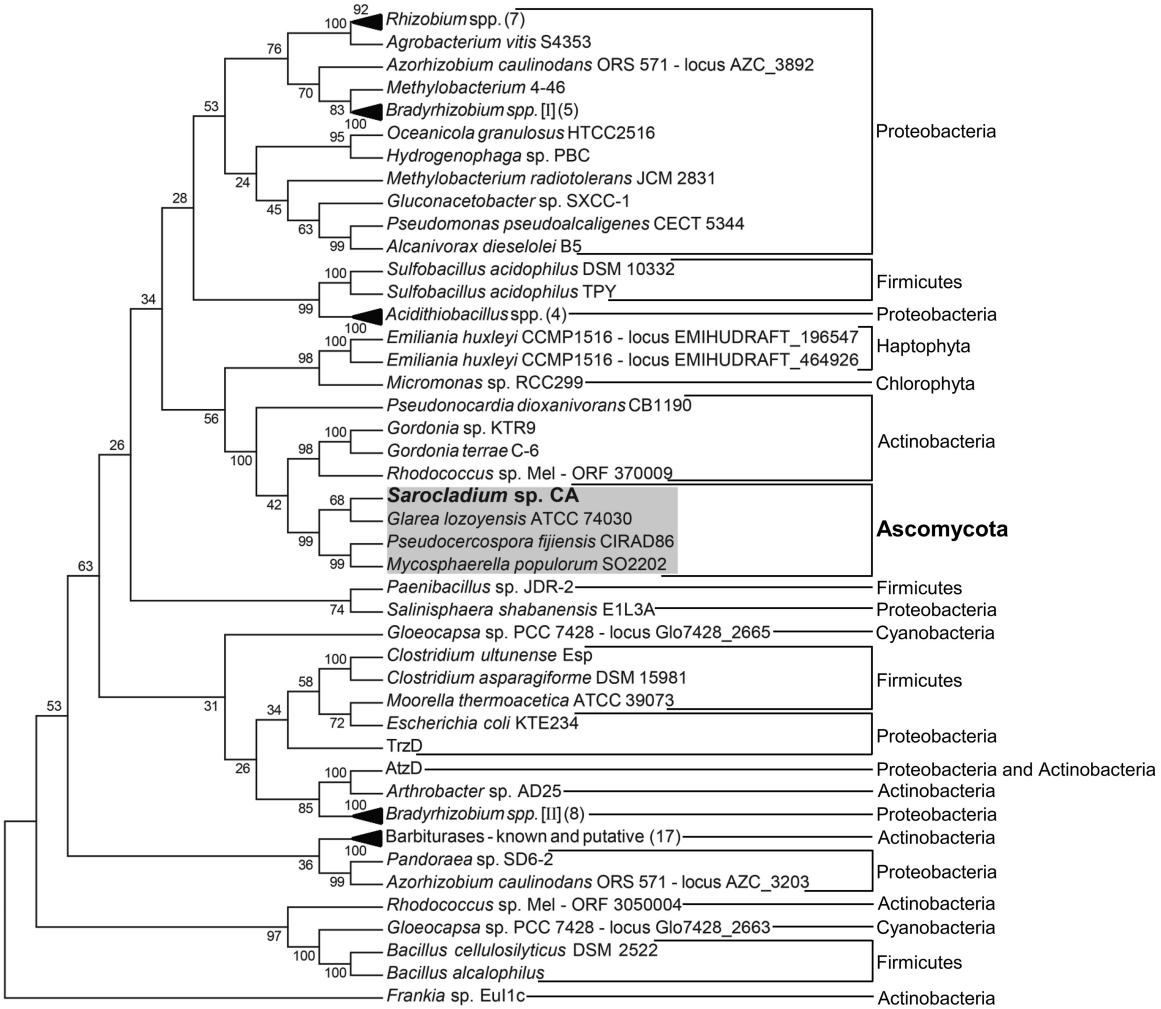

FIG 5 Maximum likelihood phylogenetic tree of cyanuric acid hydrolase/barbiturase family homologs, the consensus of 500 bootstrap replicates, rooted with the *Frankia* sp. EuI1c sequence. Bootstrap values are indicated at each node. Black triangles represent collapsed branches containing sequences from strains of the same genus or monophyletic homologs (barbiturases). The number of sequences in each set of collapsed branches is identified by an Arabic numeral in parentheses. The two separate subclades of *Bradyrhizobium* species sequences are identified by bracketed Roman numerals. Phyla of the source strains are indicated by labeled brackets or lines. The GI numbers of sequences are shown in Table S1 in the supplemental material.

Rhodococcus sp. Mel (ORF 370009) (16). This branch of seven sequences shared a node with another actinobacterial sequence (from *Pseudonocardia dioxanivorans* CB1190), and this eight-sequence branch shared a node with a branch containing the *Micromonas* and *Emiliania* sequences (Fig. 5). All of the eukaryotic sequences were placed into the same subclade within the cyanuric acid hydrolase homologs. However, the fungal sequences were more closely related to actinobacterial sequences than to the *Micromonas* and *Emiliania* sequences.

The subclade containing the seven eukaryotic sequences and the four actinobacterial sequences described above appeared consistently when different alignment (MUSCLE or ClustalW) or tree-building (maximum likelihood or neighbor-joining) algorithms were used. The arrangement of the actinobacterial sequences differed slightly in the neighbor-joining tree, with the *Pseudonocardia* sequence placed onto a branch with the *Rhodococcus* and *Gordonia* sequences (not shown). With either method, the fungal sequences were most closely related to the actinobacterial sequences, and the *Micromonas* and *Emiliania* sequences were on a separate branch at the most basal node of the subclade.

Evidence of possible horizontal gene transfer between bacteria and *Micromonas* and other algae (39, 40) and also between fungi and *Actinobacteria* (41) has been reported. The possibility of horizontal transfer of cyanuric acid hydrolase genes between bacteria and eukaryotes is suggested by the current phylogenetic tree (Fig. 5), but firm conclusions cannot be drawn due to the small set of eukaryotic homologs. Extensive genetic drift has occurred within this protein family (Table 2) (11), and absolute relationships among the cyanuric acid hydrolase homologs are difficult to assert with confidence due to low bootstrap support of several nodes in the tree (Fig. 5). Discovery of more homologs in future genome sequencing projects may help to clarify the phylogeny of eukaryotic cyanuric acid hydrolases relative to bacterial homologs.

While this study was being conducted, the first X-ray structure of a cyanuric acid hydrolase was reported (42). That study identified three serine-lysine dyads in the cyanuric acid hydrolase from

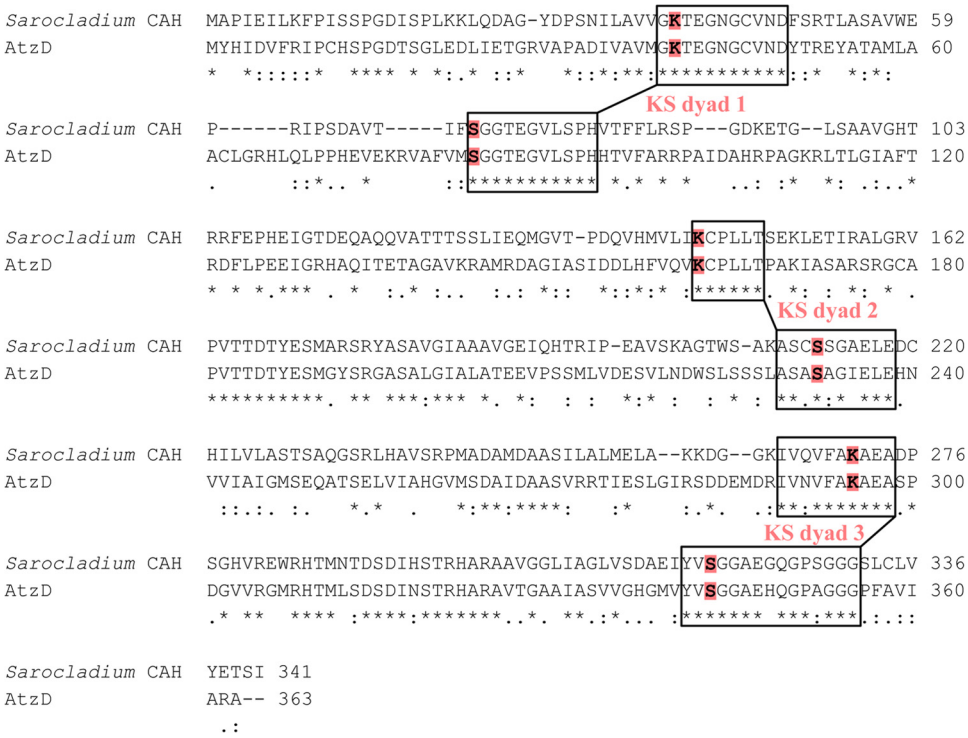

FIG 6 Alignment (ClustalW) of the *Sarocladium* sp. CA cyanuric acid hydrolase (CAH) sequence with AtzD from *Pseudomonas* sp. ADP showing conservation of the active-site lysine-serine dyads (highlighted) identified in the AtzD crystal structure reported by Peat et al. (42). The black rectangles indicate the highly conserved sequence regions surrounding the catalytic dyad residues.

Pseudomonas sp. ADP that are proposed to play a role in binding cyanuric acid and potentially promoting its hydrolysis. In this context, we looked for the presence of the three serine-lysine dyads that would be expected if the reaction mechanism of the bacterial and fungal enzymes is conserved (Fig. 6). In fact, the three serine-lysine pairs align precisely, and the regions of the dyads show 80 to 90% sequence relatedness, whereas the overall sequence relatedness is only 35 to 45%.

In conclusion, this study has identified and characterized a cyanuric acid hydrolase in a filamentous fungus. The enzyme was phylogenetically related to bacterial enzymes and displayed similar catalytic and kinetic behaviors. Cyanuric acid hydrolase activity has not been verified in other eukaryotes apart from fungi. Müller and Payot (43) reported the evolution of ^{14}C-labeled CO_2 from corn (*Zea mays*) seedlings given ^{14}C-labeled cyanuric acid. However, further study would be needed to confirm that this was due to endogenous cyanuric acid degradation. Searching the *Zea mays* genome with cyanuric acid hydrolase sequences did not identify any homologous proteins.

ACKNOWLEDGMENTS

This work was supported by a grant from the National Center for Food Protection and Defense under the Department of Homeland Security.

We thank LeeAnn Higgins and Todd Markowski at the University of Minnesota Center for Mass Spectrometry and Proteomics for their assistance with protein mass spectrometry sample preparation, analysis, and data handling. Jennifer Seffernick discovered the sequences that enabled prediction of the cyanuric acid hydrolase homolog in the *Glarea lozoyensis* ATCC 74030 genome. We gratefully acknowledge Jack Richman's expert assistance with the ^{13}C-NMR experiment.

REFERENCES

1. **Wöhler F.** 1829. On the decomposition of urea and uric acid at high temperature. Ann. Phys. Chem. **15:**619–630.
2. **Puschner B, Poppenga R, Lowenstine L, Filigenzi M, Pesavento P.** 2007. Assessment of melamine and cyanuric acid toxicity in cats. J. Vet. Diagn. Invest. **19:**616–624.
3. **Seto CT, Whitesides GM.** 1990. Self-assembly based on the cyanuric acid-melamine lattice. J. Am. Chem. Soc. **112:**6409–6411.
4. **Brown CA, Jeong KS, Poppenga RH, Puschner B, Miller DM, Ellis AE, Kang K-I, Sum S, Cistola AM, Brown SA.** 2007. Outbreaks of renal failure associated with melamine and cyanuric acid in dogs and cats in 2004 and 2007. J. Vet. Diagn. Invest. **19:**525–531.
5. **Jutzi K, Cook AM, Hütter R.** 1982. The degradative pathway of the *s*-triazine melamine. The steps to ring cleavage. Biochem. J. **208:**679–684.
6. **Sadowsky MJ, Tong Z, de Souza M, Wackett LP.** 1998. AtzC is a new member of the amidohydrolase protein superfamily and is homologous to other atrazine-metabolizing enzymes. J. Bacteriol. **180:**152–158.
7. **Cook AM, Hütter R.** 1981. *s*-Triazines as nitrogen sources for bacteria. J. Agric. Food Chem. **29:**1135–1143.
8. **Karns JS.** 1999. Gene sequence and properties of an *s*-triazine ring-cleavage enzyme from *Pseudomonas* sp. strain NRRLB-12227. Appl. Environ. Microbiol. **65:**3512–3517.
9. **Martinez B, Tomkins J, Wackett LP, Wing R, Sadowsky MJ.** 2001. Complete nucleotide sequence and organization of the atrazine catabolic plasmid pADP-1 from *Pseudomonas* sp. strain ADP. J. Bacteriol. **183:**5684–5697.
10. **Li Q, Seffernick JL, Sadowsky MJ, Wackett LP.** 2009. Thermostable cyanuric acid hydrolase from *Moorella thermoacetica* ATCC 39073. Appl. Environ. Microbiol. **75:**6986–6991.
11. **Seffernick JL, Erickson JS, Cameron SM, Cho S, Dodge AG, Richman JE, Sadowsky MJ, Wackett LP.** 2012. Defining sequence space and reaction products within the cyanuric acid hydrolase (AtzD)/barbiturase protein family. J. Bacteriol. **194:**4579–4588.
12. **Cameron SM, Durchschein K, Richman JE, Sadowsky MJ, Wackett LP.**

2011. A new family of biuret hydrolases functioning in *s*-triazine ring metabolism. ACS Catal. **2011:**1075–1082.
13. **Cheng G, Shapir N, Sadowsky MJ, Wackett LP.** 2005. Allophanate hydrolase, not urease, functions in bacterial cyanuric acid metabolism. Appl. Environ. Microbiol. **71:**4437–4445.
14. **Fruchey I, Shapir N, Sadowsky MJ, Wackett LP.** 2003. On the origins of cyanuric acid hydrolase: purification, substrates, and prevalence of AtzD from *Pseudomonas* sp. strain ADP. Appl. Environ. Microbiol. **69:**3653–3657.
15. **Stamper DM, Krzycki JA, Nicomrat D, Traina SJ, Tuovinen OH.** 2005. Ring-cleaving cyanuric acid amidohydrolase activity in the atrazine-mineralizing *Ralstonia basilensis*. Biocatal. Biotransformation **23:**387–396.
16. **Dodge AG, Wackett LP, Sadowsky MJ.** 2012. Plasmid localization and organization of melamine degradation genes in *Rhodococcus* sp. strain Mel. Appl. Environ. Microbiol. **78:**1397–1403.
17. **Kim GJ, Kim HS.** 1998. Identification of the structural similarity in the functionally related amidohydrolases acting on the cyclic amide ring. Biochem. J. **330:**295–302.
18. **Soong CL, Ogawa J, Sakuradani E, Shimizu S.** 2002. Barbiturase, a novel zinc-containing amidohydrolase involved in oxidative pyrimidine metabolism. J. Biol. Chem. **277:**7051–7058.
19. **Vogels GD, Van der Drift C.** 1976. Degradation of purines and pyrimidines by microorganisms. Bacteriol. Rev. **40:**403–468.
20. **Jensen HL, Abdel-Ghaffar AS.** 1969. Cyanuric acid as nitrogen source for micro-organisms. Arch. Microbiol. **67:**1–5.
21. **Wolf DC, Martin JP.** 1975. Microbial decomposition of ring-^{14}C-atrazine, cyanuric acid, and 2-chloro-4,6-diamino-s-triazine. J. Environ. Qual. **4:**134–139.
22. **Zeyer J, Hütter R, Mayer P.** June 1981. Process for the degradation of cyanuric acid. US patent 4,274,955.
23. **Myśków W, Lasota T, Stachyra A.** 1983. Cyanuric acid—a *s*-triazine derivative as a nitrogen source for some soil microorganisms. Acta Microbiol. Pol. **32:**177–183.
24. **Seffernick JL, Johnson G, Sadowsky MJ, Wackett LP.** 2000. Substrate specificity of atrazine chlorohydrolase and atrazine-catabolizing bacteria. Appl. Environ. Microbiol. **66:**4247–4252.
25. **Smolin EM, Rapoport L.** 1959. *s*-Triazines and derivatives, p 269–308. *In* Weissberger A (ed), The chemistry of heterocyclic compounds. Interscience Publishers Inc, New York, NY.
26. **Tomasek PH, Karns JS.** 1989. Cloning of a carbohydrolase gene from *Achromobacter* sp. strain WM11 and its expression in Gram-negative bacteria. J. Bacteriol. **173:**4038–4044.
27. **White T, Bruns T, Lee S, Taylor J.** 1990. Amplification and direct sequencing of fungal ribosomal RNA genes for phylogenetics, p 315–322. *In* Innis MA, Gelfand DH, Sninsky JJ, White TJ (ed), PCR protocols: a guide to methods and applications. Academic Press Inc, San Diego, CA.
28. **Altschul SF, Gish W, Miller W, Myers EW, Lipman DJ.** 1990. Basic local alignment search tool. J. Mol. Biol. **215:**403–410.
29. **Larkin MA, Blackshields G, Brown NP, Chenna R, McGettigan PA, McWilliam H, Valentin F, Wallace IM, Wilm A, Lopez R, Thompson JD, Gibson TJ, Higgins DG.** 2007. ClustalW and ClustalX version 2. Bioinformatics **23:**2947–2948.
30. **Tamura K, Peterson D, Peterson N, Stecher G, Nei M, Kumar S.** 2011. MEGA5: molecular evolutionary genetics analysis using maximum likelihood, evolutionary distance, and maximum parsimony methods. Mol. Biol. Evol. **28:**2731–2739.
31. **Edgar RC.** 2004. MUSCLE: multiple sequence alignment with high accuracy and high throughput. Nucleic Acids Res. **32:**1792–1797.
32. **Bradford MM.** 1976. A rapid and sensitive method for the quantitation of microgram quantities of protein utilizing the principle of protein-dye binding. Anal. Biochem. **72:**248–254.
33. **Ishihama Y, Rappsilber J, Mann M.** 2006. Modular stop and go extraction tips with stacked disks for parallel and multidimensional peptide fractionation in proteomics. J. Proteome Res. **5:**988–994.
34. **Lin-Moshier Y, Sebastian PJ, Higgins L, Sampson ND, Hewitt JE, Marchant JS.** 2013. Re-evaluation of the role of calcium homeostasis endoplasmic reticulum protein (CHERP) in cellular calcium signaling. J. Biol. Chem. **288:**355–367.
35. **Giegerich R, Meyer F, Schleiermacher C.** 1996. GeneFisher—software support for the detection of postulated genes. Proc. Int. Conf. Intell. Syst. Mol. Biol. **4:**68–77.
36. **Okamura T, Kigasawa K.** 1994. Re-evaluation of the colorimetric assay for cytidine deaminase activity. Prenat. Diagn. **14:**213–218.
37. **Summerbell RC, Gueidan C, Schroers H-J, Hoog GS, de Starink M, Rosete YA, Guarro J, Scott JA.** 2011. *Acremonium* phylogenetic overview and revision of *Gliomastix*, *Sarocladium*, and *Trichothecium*. Stud. Mycol. **68:**139–162.
38. **Cook AM, Beilstein P, Grossenbacher H, Hütter R.** 1985. Ring cleavage and degradative pathway of cyanuric acid in bacteria. Biochem. J. **231:**25–30.
39. **McDonald SM, Plant JN, Worden AZ.** 2010. The mixed lineage nature of nitrogen transport and assimilation in marine eukaryotic phytoplankton: a case study of *Micromonas*. Mol. Biol. Evol. **27:**2268–2283.
40. **Schönknecht G, Chen WH, Ternes CM, Barbier GG, Shrestha RP, Stanke M, Bräutigam A, Baker BJ, Banfield JF, Garavito RM, Carr K, Wilkerson C, Rensing SA, Gagneul D, Dickenson NE, Oesterhelt C, Lercher MJ, Weber AP.** 2013. Gene transfer from bacteria and archaea facilitated evolution of an extremophilic eukaryote. Science **339:**1207–1210.
41. **Schmitt I, Lumbsch HT.** 2009. Ancient horizontal gene transfer from bacteria enhances biosynthetic capabilities of fungi. PLoS One **4:**e4437. doi:10.1371/journal.pone.0004437.
42. **Peat TS, Balotra S, Wilding M, French NG, Briggs LJ, Panjikar S, Cowieson N, Newman J, Scott C.** 2013. Cyanuric acid hydrolase: evolutionary innovation by structural concatenation. Mol. Microbiol. **88:**1149–1156.
43. **Müller PW, Payot PH.** 1966. Fate of ^{14}C-labelled triazine herbicides in plants, p 61–70. *In* Isotopes in weed research. Proceedings of the Symposium on the Use of Isotopes in Weed Research. International Atomic Energy Agency, Vienna, Austria.